ANL/MSD/CP-99687

58930-00-105
58906-00-105
85088-80-105

Conference Paper

Top Seeded Growth and Joining of Bulk YBCO

H. Zheng, B.W. Veal, A. Paulikas, R. Nikolova, U. Welp, H. Claus, and G.W. Crabtree

Materials Science Division
Argonne National Laboratory, Argonne, IL 60439

Institute of Physics Conference Series, Proceedings of the European Conference on Applied Superconductivity (EUCAS 99), Sitges, Spain, Sep. 14-17, 1999

Work supported by the U.S. Department of Energy, Basic Energy Sciences-Materials Sciences under contract #W-31-109-ENG-38 and by the NSF Science and Technology Center for Superconductivity, Contract #DMR 91-20000 (HZ).

DISCLAIMER

top seeded growth and joining of bulk YBCO

H Zheng, B W Veal, A Paulikas, R Nikolova, U Welp, H Claus and G W Crabtree

Materials Science Division, Argonne National Laboratory, Argonne Illinois 60439

ABSTRACT: We report (i) systematic studies of the growth rate for melt textured YBCO, (ii) top seeding growth techniques to determine the minimum seed size, and (iii) joining techniques for melt textured YBCO, enabling the fabrication of large single domain structures of arbitrary shape. Seeded growth of YBCO occurs in a narrow temperature window about 20°C below the peritectic decomposition temperature. Successful top seeding depends on the size of the NdBCO seed crystal. Small seeds are eventually dissolved in the melt before nucleation occurs, while large seeds regularly produce single domain monoliths. Joining techniques based on seeding of low melting point Tm123/Y211 filler material by neighboring YBCO are described. Magneto-optical images of the YBCO/TmBCO/YBCO assembly show no detectable penetration of magnetic field at the joints.

The high critical current densities obtainable in melt-textured $YBa_2Cu_3O_x$ (YBCO or Y123) [Murakami 1992, Salama and Lee 1994, Zhukov et al 1995] have made this material attractive for applications in motors, fault current limiters, and trapped field magnets. However, for successful industrial applications, the process parameters need to be further optimized. In this paper we report three such optimization studies: conditions for successful seeding, optimal growth condition, and assembling of large superconducting structures by a welding technique.

The melt texturing was achieved by a top-seeding method [Marinel et al 1997, Meignan et al 1997]. Typically, 10 and 26 mm diameter cylindrical samples were produced from Y123 and Y211 powders (99.9% purity, Superconductive Components) mixed in a weight ratio of 75:25. The mixture was pressed into cylindrical pellets at pressures of 100 MPa. A Nd123 seed crystal was placed on top of a pressed pellet with the crystal c-axis parallel to the cylinder axis. The samples were then heated to 1030°C, above the peritectic point, and were held there for two hours. The samples were then rapidly cooled to 1000°C, followed by a slow cooling ramp (0.5 - 1°C/hr) to a temperature of 970°C, or lower, for solidification. Samples were then furnace cooled to room temperature. Oxygenation was performed at 450°C for 10 days in flowing oxygen.

It was previously observed that seeding was sometimes unsuccessful due to dissolution of the seed crystal. To determine the minimum thickness of crystals needed for successful seeding, we measured the dissolution rate at 1030°C, the highest hold temperature. Seed crystals with different thickness were placed on top of the pellets, the pellets were heated to 1030°C and held for time intervals between 1.5 and 9 hrs. The temperature was then dropped rapidly to 995°C where it was held (typically for 35 hrs) to facilitate seeded growth. When seeding has occurred, it is easily identified by a square growth pattern surrounding the seed. Fig. 1 summarizes the results of this study. Plotted is the seed thickness vs. the hold time at 1030°C. Open circles designate seeding failure, solid circles designate successfully seeded samples. A clear demarcation line separating conditions for seeding success and seeding failure is seen in Fig. 1 (dotted line). This line corresponds to a dissolution rate of the seed crystals of 30 μm/h. Using seed crystal thickness above this demarcation line leads to near 100% seeding success.

To further optimize the melt-texturing process, it is important to identify the temperature window where rapid melt-textured growth takes place. To this purpose, the samples solidified at constant temperature between 960 and 1010°C for 6 hours after initially melting them for 2 hours at 1030°C. After the texturing process, the samples were fast cooled to room temperature and the size of the seeded region determined. The growth rate determined this way is plotted in Fig. 2 for Y123/Y211 and Tm123/Y211. For Y123/Y211 the growth window is only about 10°C wide with a maximum growth rate of 1.5 mm/h at T_{max} = 993°C. The plotted points are determined from the dimension of the central growth region seeded by the Nd crystal. The maximum in the size of the seeded region reflects a balance between the growth rate and the spontaneous secondary nucleation rate. Above T_{max} the secondary nucleation rate is low and Fig. 2 reflects the monotonically increasing growth rate with decreasing temperature. Below T_{max} the size of the seeded growth region is limited by spontaneous secondary nucleation at sites remote from the seed crystal. The net result is that the region of seeded growth surrounding the Nd seed crystal goes through a maximum as shown in Fig. 2. For growth below T_{max}, rapidly advancing growth from multiple competing domains result in an ill-defined region of seeded growth at the center. Clearly, a knowledge of growth temperature window is needed for optimization of melt-texture growth. Fig. 2 also shows the growth window for Tm123/Y211 melt texturing. All of the characteristic temperatures for this material, such as melting temperature and T_{max}, are about 20°C lower than those for Y123/Y211. Similar optimization growth windows can easily be established for other RE123 compounds.

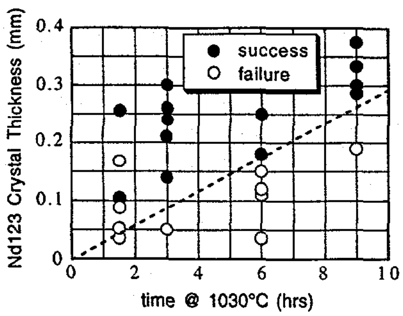

Fig. 1 Seed crystal thickness required for successful seeding, see text.

Spontaneous secondary nucleation will eventually limit the maximum size of single domain samples to not more than several inches diameter [Zheng 1999]. However, large monolithic components are needed in the construction of many HTS devices. If small single domain units could be reliably welded with high current superconducting joints, then custom monolithic units of arbitrary size and shape could be assembled from small single domain building blocks which can be inexpensively fabricated [Zheng 1999].

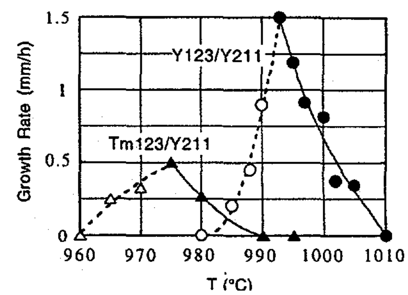

Fig. 2 Seeded growth rate vs. temperature

To achieve this goal, we used Tm123/Y211 as flux to join two monolithic Y123/Y211 pieces together. As mentioned above, the peritectic decomposition temperature of the Tm123/Y211 mix is about 20°C lower than that of Y123/Y211. In the welding operation, the assembled Y123/Y211 monoliths and the Tm123/Y211 pressed powder spacer are heated to a temperature intermediate between the two decomposition temperatures. The spacer material decomposes to a two-phase mixture of liquid and dispersed solid green phase while the YBCO parts remain solid and undeformed. The liquid will wet (and mildly attack) the exposed Y123 surfaces to be joined. With cooling, the textured YBCO mating parts serve as seeds to texture the Tm123/Y211 spacer material. With this procedure, a nearly seamless superconducting joint can be obtained. An example is shown in Fig. 3. A melt-textured YBCO puck was cut in half and welded back together with a Tm123/Y211 layer as shown schematically on the left. On the right is a magneto-optical picture of a small slice containing the weld, as indicated. This picture was taken in a magnetic field of a few hundred gauss. The brighter region near the surface of the slice indicates field penetration into the sample. This penetration is uniform across the imaged slice, demonstrating that at the joints (marked by the arrows) the field penetrates no further than in the bulk [Zheng 1999]. This clearly demonstrates that the critical current of the joint is comparable to that of the bulk.

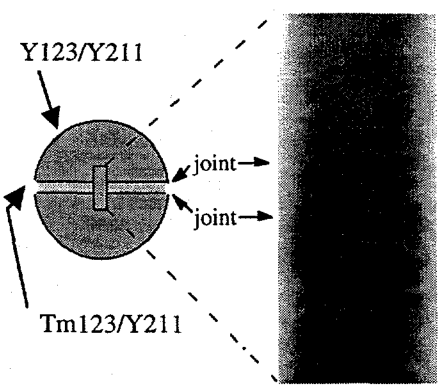

Fig. 3 Left side: schematic welding arrangement. Right side: magneto-optical image of the slice as indicated (see text)

This work was supported by the US Department of Energy, Office of Basic Energy Sciences - Materials Sciences, Contract No. W - 31 - ENG - 38 (BWV, AP, RN, UW, GWC, HC) and the NSF Science and Technology Center for Superconductivity, Contract No. DMR 91-20000 (HZ).

Marinel S et al. 1997 Supercond. Sci. Technol. **10** 147
Meignan P et al. 1997 Supercond. Sci. Technol. **10** 109
Murakami M 1992 Supercond. Sci. Technol. **5** 18
Salama K and Lee D F 1994 Supercond. Sci. Technol. **7**, 177
Zheng H et al. 1999 Physica C, in press
Zhukov A A et al. 1995 Phys. Rev. B **51** 12704